

The global distribution and spread of the mobilized colistin resistance gene *mcr-1*

Ruobing Wang^{1*}, Lucy van Dorp^{2*}, Liam Shaw^{2*}, Phelim Bradley³, Qi Wang¹, Xiaojuan Wang¹, Longyang Jin¹, Qing Zhang⁴, Yuqing Liu⁴, Adrien Rieux⁵, Thamarai Dorai-Schneiders⁶, Lucy Anne Weinert⁷, Zamin Iqbal⁹, Xavier Didelot⁸, Hui Wang¹ and Francois Balloux²

¹ Department of Clinical Laboratory, Peking University People's Hospital, Beijing, 100044, China

² UCL Genetics Institute, University College London, Gower Street, London WC1E 6BT, UK

³ Wellcome Trust Centre for Human Genetics, University of Oxford, Oxford OX3 7BN, UK

⁴ Institute of Animal Science and Veterinary Medicine, Shandong Academy of Agricultural Sciences, Shandong Province, Jinan, 250100, China

⁵ UMR PVBMT, CIRAD, 97410 St Pierre, Reunion, France

⁶ Division of Infection and Pathway Medicine, 49 Little France Crescent, Edinburgh EH16 4SB, UK

⁷ Department of Veterinary Medicine, Cambridge CB3 0ES, UK

⁸ Department of Infectious Disease Epidemiology, Imperial College London, Norfolk Place, 21 London W2 1PG, UK

⁹ European Molecular Biology Laboratory, European Bioinformatics Institute (EMBL-EBI), Wellcome Genome Campus, Cambridge CB10 1SD, UK

Correspondence: Hui Wang: wanghui@pkuph.edu.cn and Francois Balloux: f.balloux@ucl.ac.uk

Abstract

Colistin represents one of the very few available drugs for treating infections caused by carbapenem resistant Enterobacteriaceae (CRE). As such, the recent plasmid-mediated spread of the mobilized colistin resistance gene *mcr-1* poses a significant public health threat requiring global monitoring and surveillance. In this work, we characterize the global distribution of *mcr-1* using a dataset of 457 *mcr-1* positive sequenced isolates consisting of currently publicly available *mcr-1* carrying sequences combined with an additional 110 newly sequenced *mcr-1* positive isolates from China. We find *mcr-1* in a diversity of plasmid backgrounds but identify an immediate background common to all *mcr-1* sequences. Our analyses establish that all *mcr-1* elements in circulation descend from the same initial mobilization of *mcr-1* by an IS*Apl1* transposon in the mid 2000s (2002-2008; 95% higher posterior density), followed by a dramatic demographic expansion, which led to its current global distribution. Our results provide the first systematic phylogenetic analysis of the origin and spread of *mcr-1*, and emphasize the importance of understanding the movement of mobile elements carrying antibiotic resistance genes across multiple levels of genomic organization.

Introduction

Colistin was largely abandoned as a treatment for bacterial infections in the 1970s due to its high toxicity and low renal clearance, but has been reintroduced in recent years as an antibiotic of 'last resort' against multi-drug-resistant (MDR) infections¹. It is therefore alarming that the prevalence of resistance to colistin has become a significant concern, following the identification of plasmid-mediated colistin resistance conferred by the *mcr-1* gene in late 2015². Colistin resistance is emblematic of the growing problems of antimicrobial resistance worldwide.

Up until 2015, resistance to colistin had only been linked to mutational and regulatory changes mediated by chromosomal genes^{3,4}. The mobilized colistin gene *mcr-1* was first described in a plasmid carried by an *Escherichia coli* isolated in China in April 2011². The presence of colistin resistance on mobile genetic elements poses a significant public health risk, as these can spread rapidly by horizontal transfer, and may entail a lower fitness cost⁵. At the time of writing, *mcr-1* has been identified in numerous countries across five continents. Significantly, *mcr-1* has also been observed on plasmids containing other antimicrobial resistance genes such as carbapenemases⁶⁻⁸ and extended-spectrum β -lactamases (ESBL)⁹⁻¹¹.

The *mcr-1* element has been characterized in a variety of genomic backgrounds, consistent with the gene being mobilized by a transposon¹²⁻¹⁶. To date, *mcr-1* has been observed on a wide variety of plasmid types, including IncI2, IncHI2, and IncX4¹⁵. Intensive screening efforts for *mcr-1* have found it to be highly prevalent in a number of environmental settings, including the Haihe River in China¹⁷, recreational water at public urban beaches in Brazil¹⁸, and faecal samples from otherwise healthy individuals^{19,20}. While both Brazil and China have now banned the use of colistin in agriculture, the evidence that *mcr-1* can spread within hospital environments even in the absence of colistin use¹⁹ as well as in the community²⁰ raises the possibility that the spread of *mcr-1* will not be contained by these bans.

The global distribution of *mcr-1* over at least five continents is well documented, but little is known about its origin, acquisition, emergence, and spread. In this study, we aim to shed light on these fundamental issues using whole genome sequencing data from 110 novel *mcr-1* positive isolates from China in conjunction with an extensive collection of publicly available sequence data sourced from the NCBI repository as well as the Short Read Archive (SRA).

Our data and analyses support an initial single mobilization event of *mcr-1* by an IS*ApI1*-*mcr-1*-orf-IS*ApI1* transposon around 2006. The transposon was immobilized on several plasmid backgrounds following the loss of the flanking IS*ApI1* elements, and

spread through plasmid transfer. The current distribution of *mcr-1* points to a possible origin in Chinese livestock. Our results illustrate the complex dynamics of antibiotic resistance genes across multiple embedded genetic levels (transposons, plasmids, bacterial lineages and bacterial species), previously described as a nested “Russian doll” model of genetic mobility²¹.

Results

Dataset

We compiled a global dataset of 457 *mcr-1* positive isolates (Figure 1A), including 110 new whole genome sequences (WGS) from China, of which 107 were sequenced with Illumina short reads and three with PacBio long read technology. 195 isolates were sourced from publicly available assemblies in the NCBI sequence repository (73 completed plasmids, 1 complete chromosome, 121 assemblies). A further 153 sequences were sourced from the Short Read Archive (NCBI-SRA), after being identified as *mcr-1* positive using a k-mer index of a snapshot of the SRA as of December 2016 (see Methods). The whole dataset consists of 256 short-read datasets, 6 long-read PacBio WGS, 121 draft assemblies, and 74 completed assemblies.

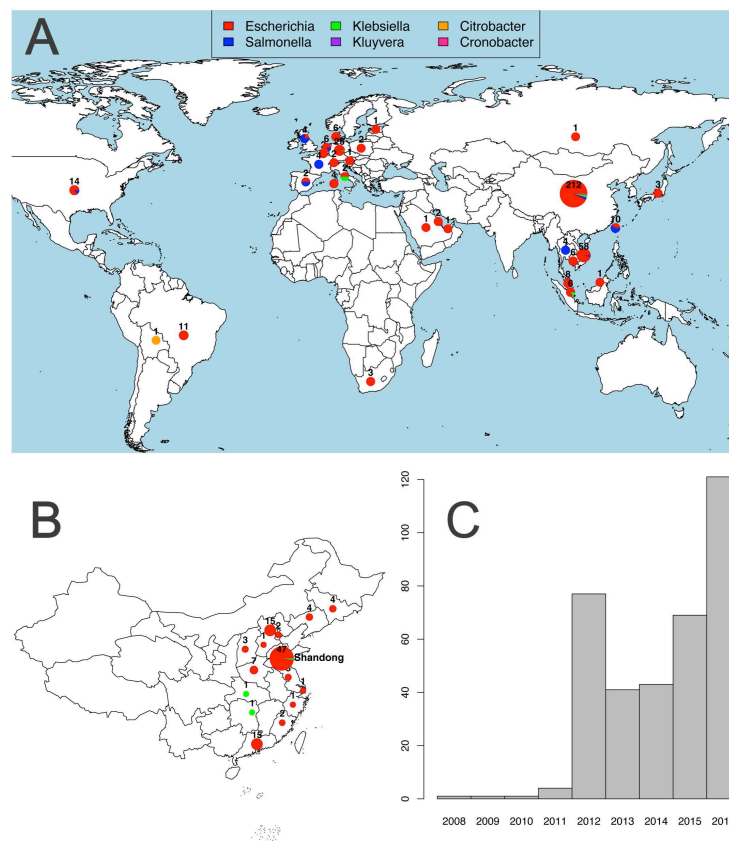


Figure 1. Overview of the *mcr-1* positive isolates included. **A.** Global map of *mcr-1* positive isolates included coloured by genus with the number and size of pies providing the sample size per location; **B.** Map of novel Chinese isolates sequenced for this study; **C.** Histogram of sampling dates (years) of the isolates.

Isolates carrying *mcr-1* were identified from 31 countries (Figure 1A). The countries with the largest numbers of *mcr-1* positive samples are China (212), Vietnam (58) and Germany (25). Within China, nearly half (45%) of positive isolates stem from Shandong province (Figure 1B). The vast majority of *mcr-1* positive isolates belong to *Escherichia coli* (411), but the dataset also comprises *mcr-1* positive isolates from another seven bacterial species: *Salmonella enterica* (29), *Klebsiella pneumoniae* (8), *Escherichia fergusonii* (2), *Kluyvera ascorbata* (2), *Citrobacter braakii* (2), *Cronobacter sakazakii* (1) and *Klebsiella aerogenes* (1) (Figure 1A). The majority of isolates for which sampling dates were available (80%), were collected between 2012 and 2016, with the oldest available isolates dating back to 2008 (Figure 1C).

The large number of *mcr-1* positive isolates from China, and the high incidence in Shandong province can be largely ascribed to the inclusion of our 110 newly sequenced isolates including 49 from Shandong and to another 37 isolates from a previous large sequencing effort¹³. However, even after discounting the isolates from these two sources, China remains, together with Vietnam one of the two countries with the highest number of sequenced *mcr-1* positive isolates.

Evolutionary model

It has been proposed that *mcr-1* is mobilized by a composite transposon formed of a ~2,600bp region containing *mcr-1* (1,626bp) and a putative open reading frame encoding a PAP2 superfamily protein (765bp), flanked by two IS*Ap11* insertion sequences¹². IS*Ap11* is a member of the IS30 family of insertion sequences, which utilize a 'copy-out, paste-in' mechanism with a targeted transposition pathway requiring the formation of a synaptic complex between an inverted repeat (IR) in the transposon circle and an IR-like sequence in the target. Snesrud and colleagues¹² hypothesized that after the initial formation of such a composite transposon, these insertion sequences would have been lost over time, leading to the stabilization of *mcr-1* in a diverse range of plasmid backgrounds (Figure 2). In the following, we sought to test this model by performing an explicit phylogenetic analysis of the region surrounding *mcr-1* using our comprehensive global dataset.

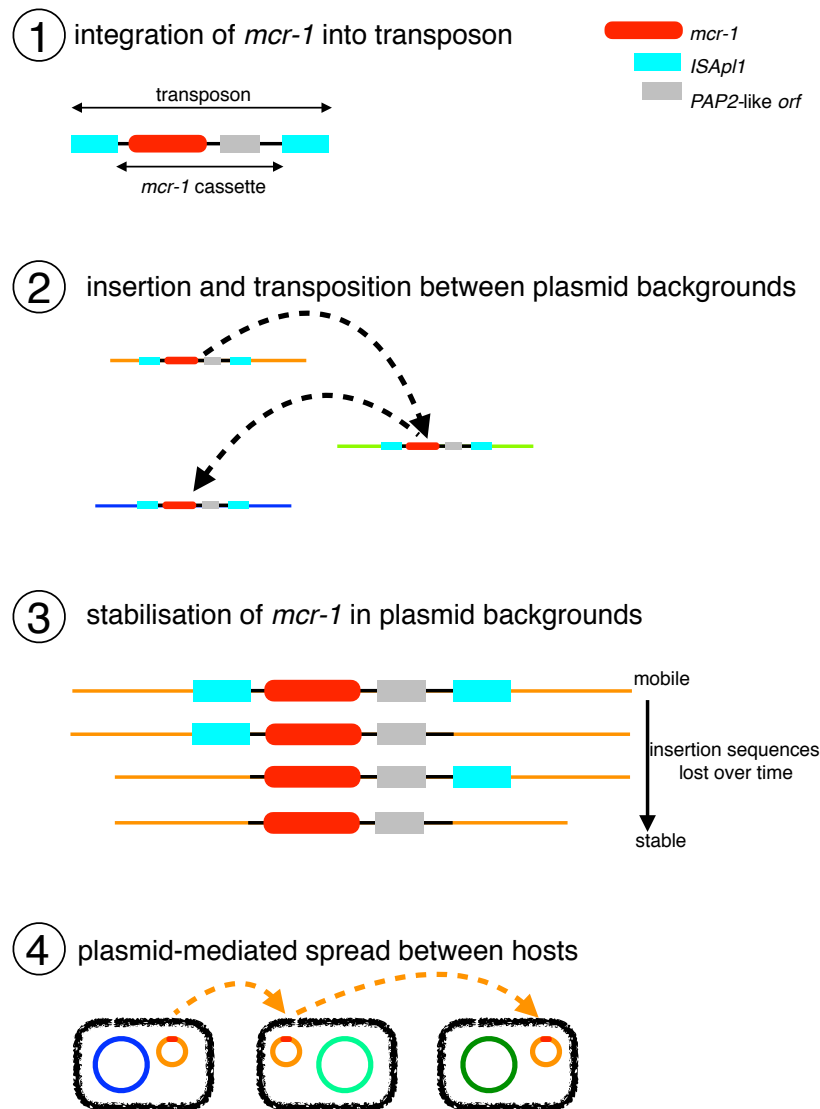


Figure 2. Schematic representation of the evolutionary model for the steps in the spread of the *mcr-1* gene. (1) The formation of the original composite transposon, followed by (2) transposition between plasmid backgrounds and (3) stabilisation via loss of ISAp1 elements before (4) plasmid-mediated spread.

Immediate genomic background of mcr-1

If there had been a unique formation event for the composite transposon, followed by progressive transposition and loss of insertion sequences, we would expect to be able to identify a common immediate background region for *mcr-1* in all samples. Indeed, we were able to identify and align a shared region or remnants of it in all 457 sequences surrounding *mcr-1* (see Methods), supporting a single common origin for all *mcr-1* elements sequenced to date (Figure 3a). The majority of the sequences contained no trace of *ISAp11* (n=260) indicating that the *mcr-1* transposon had been completely stabilized in their genomic background. 42 sequences contained indication of the presence of *ISAp11* both upstream and downstream, either in full copies (n=16), a full copy upstream and a partial copy downstream (n=7), a partial copy upstream and a full copy downstream (n=1), or partial copies upstream and downstream (n=18). Some sequences only had *ISAp11* present upstream as a complete (n=55) or partial (n=99) sequence, and one sequence had only a partial downstream *ISAp11* element. The downstream copy of *ISAp11* was inverted in some sequences (n=3) and some sequences had full copies of *ISAp11* present elsewhere on the same contig (n=7), consistent with its high observed activity in transposition²².

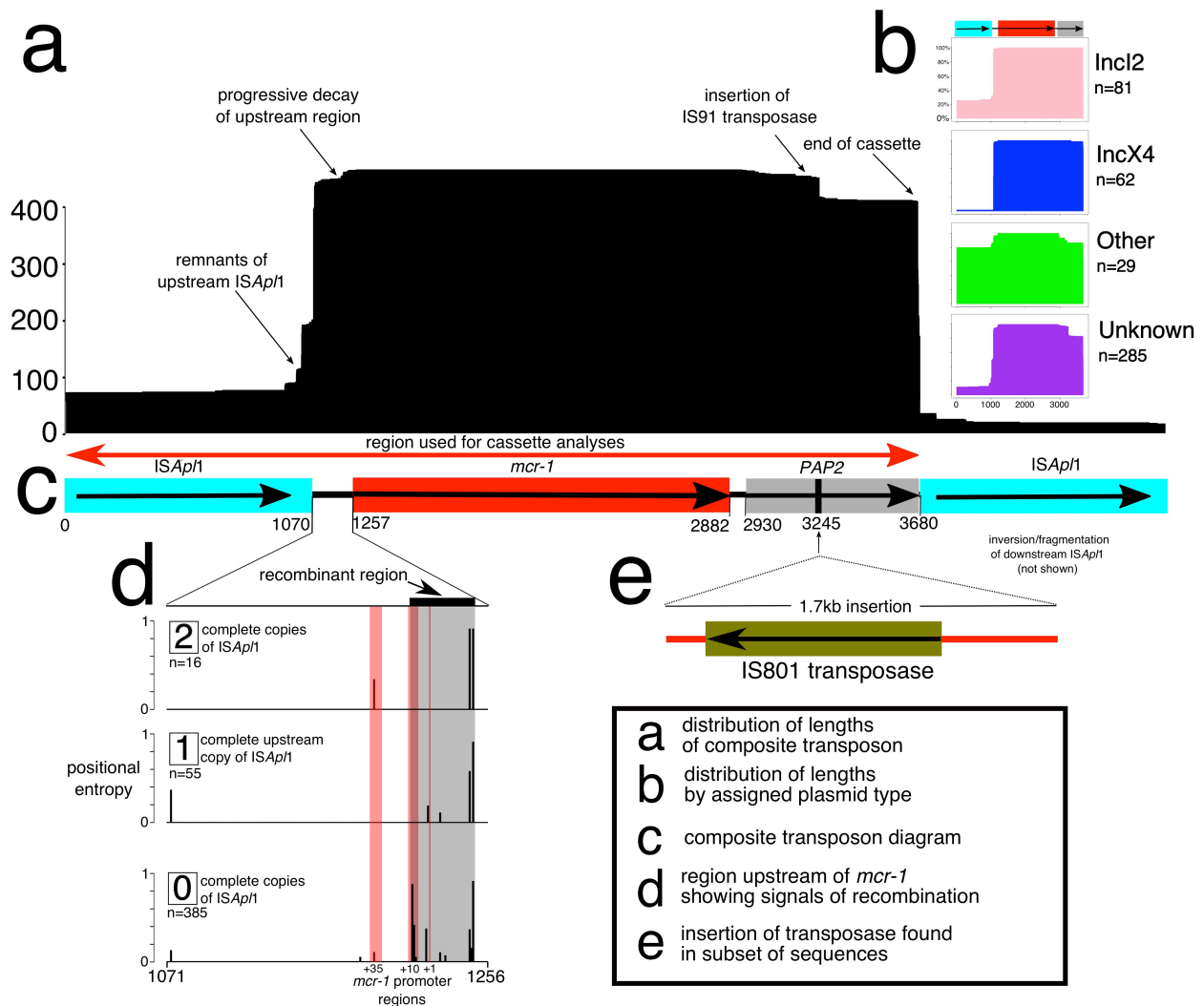


Figure 3. The genetic element carrying *mcr-1* is a composite transposon and is alignable across our global dataset. (a) Length distribution of the alignment across sequences. (b) Length distribution subset by plasmid type. (c) The composite transposon, consisting of ISAp1, *mcr-1*, a PAP2 *orf*, and ISAp1. The region indicated by the red arrow was used in phylogenetic analyses, after the removal of recombination. (d) The 186bp region upstream of *mcr-1* showed strong signals of recombination (grey box) that coincided with the promoter regions of *mcr-1* (red box), and this diverse region was removed from the subsequent alignment. (e) 28 sequences from Vietnam had a 1.7kb insertion containing a region with >99% sequence identity to IS801 transposase, suggesting subsequent rearrangement after initial mobilization.

Further inspection of the transposon alignment revealed that the 186bp region between the 3' end of the upstream ISAp1 and *mcr-1* contained IR-like sequences similar to the IRR and IRL of ISAp1 (respectively: 93-142bp, 23/50 identity; and 125-175bp, 21/50 identity). The most variable positions in this 186bp region were at 177bp and 142bp, approximately coinciding with the end of the alignment with the IRs and were more

variable in sequences lacking IS*Ap1*, suggesting possible loss of function of the transposition pathway associated with IS*Ap1* (Figure 3d). Some of these SNPs occurred in a stretch previously identified as the promoter region for *mcr-1*²³, and this region showed strong signals of recombination. A small number of sequences (3%) had SNPs present in *mcr-1* itself. These tended to be at the upstream/5' end of the sequence, particularly in the first three positions. A subset of the sequences from Vietnam (n=28) included a secondary 1.7kb insertion downstream of *mcr-1* containing an IS801 transposase, indicating subsequent rearrangements involving this region after initial mobilization of the transposon (Figure 3e).

To reconstruct the phylogenetic history of the composite *mcr-1* transposon, we created a sequence alignment for 457 sequences (Figure 3c) after removal of recombinant regions identified with ClonalFrameML, including the region immediately upstream of *mcr-1* between positions 1,212-1,247 (Figure 3d). A midpoint-rooted maximum parsimony phylogeny showed that there was a dominant sequence type with subsequent diversification, likely indicating the ancestral form of the composite transposon (Figure 4).

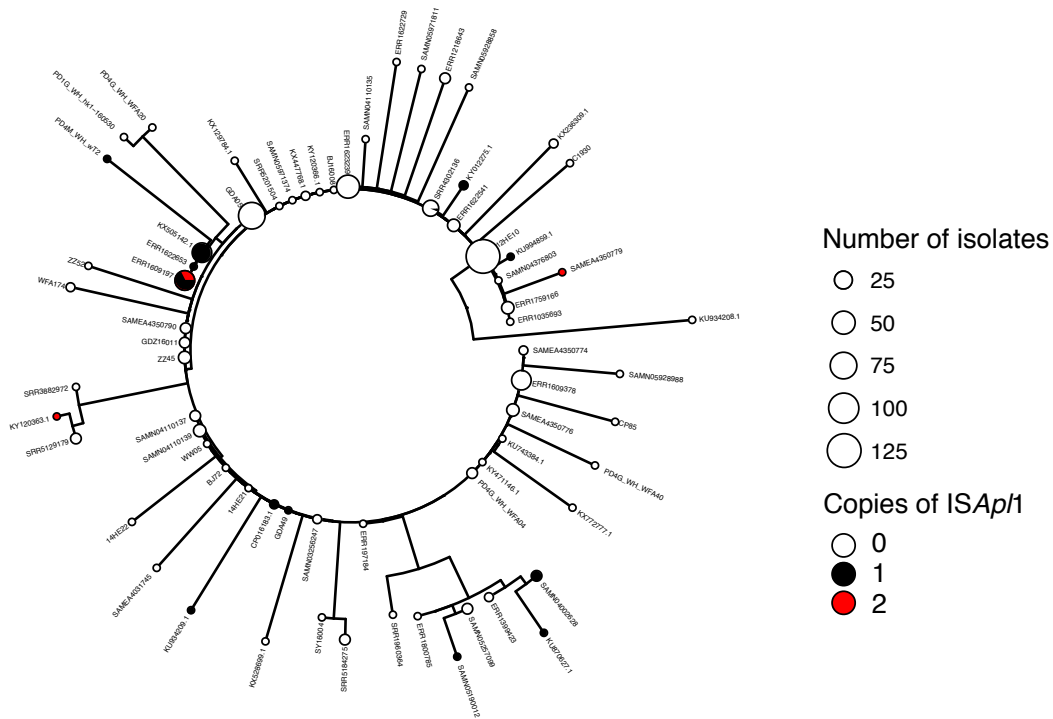


Figure 4. Phylogeny of the *mcr-1* composite transposon indicates a dominant sequence type with subsequent diversification. Midpoint-rooted maximum parsimony phylogeny based on the 3,522bp alignment of 457 sequences (recombinant regions removed). Size of points indicates the number of identical sequences, with a representative sequence for each shown next to each tip.

A Bayesian dating approach (BEAST) was applied to infer a timed phylogeny of the maximal alignable region of the *mcr-1* carrying transposon (see Methods). Based on this 3,522 site alignment we infer a common ancestor for 364 dated isolates in 2006 (Figure S1; 2002-2008 95% HPD strict clock, coalescent model) with a mutation rate around 7.51×10^{-5} substitutions per site per year (Table S1). There was no clear overall geographic clustering in the maximum clade credibility tree (Figure S2).

Wider genomic background of mcr-1

Next, we explored the wider genomic background upstream and downstream of the conserved transposon sequences. We had sufficiently long assembled contigs for 172 isolates to identify plasmid types based on co-occurrence with plasmid replicons (see Methods) and identified *mcr-1* in 13 different plasmid backgrounds. IncI2 and IncX4

were the dominant plasmid types, accounting for 47% and 36% of the isolates, respectively (Figure 5). One isolate in our dataset was located on a chromosome.

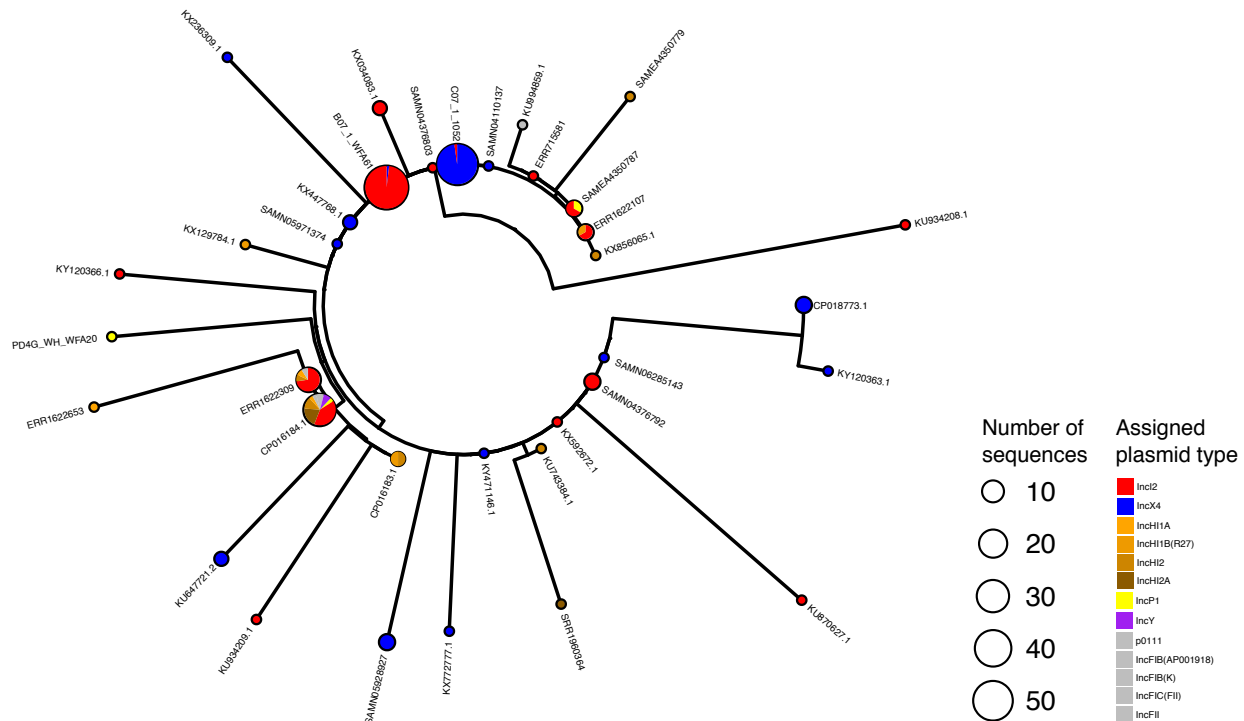


Figure 5. The distribution of plasmid types shown on the transposon phylogeny. Maximum parsimony tree (homoplastic sites removed, mid-point rooted, as in Figure 4) based on the composite transposon alignment for 172 sequences containing a plasmid replicon on the same contig i.e. those with an assigned plasmid type (color). Incl2 and IncX4 are the most common plasmid types. An example sequence ID is shown for each unique sequence.

The distribution of transposons carrying one or two copies of *ISAp11* was highly heterogeneous across these plasmid types. For example, sequences with one or two copies of *ISAp11* were found on 11 and seven types, respectively, which supports their mobility compared to those without *ISAp11*, which were found in six plasmid types. Of the contigs carrying one copy of *ISAp11*, 65% were found in Incl2 plasmids, and 43% of contigs carrying two copies of *ISAp11* belonged to IncH12 plasmids. Conversely, the common IncX4 plasmids carried only one transposon with two copies of *ISAp11* and none with a single copy of the element.

We identified two extended plasmid backbone sequences that could be aligned. The first such alignment encompasses a shared sequence of 7,161bp between 108 plasmid backgrounds and has been previously referred to as 'Type A'¹³. These sequences contain 54 sequences co-occurring with an Incl2 replicon, with 54 of unknown plasmid

type, and encompass a large fraction of the genetic diversity found in the *mcr-1* transposon, although a large proportion (9/108) belonged to the dominant sequence type (i.e. B07_1_WFA61 in Figure 4). The second alignment is 34,761 bp long and is common to nine IncX4 plasmids and partly overlaps with a background previously defined as ‘Type D’¹³.

We applied BEAST to infer a timed phylogeny for each of these alignable regions after removal of SNPs showing evidence of recombination. For the IncI2 background we infer that a common ancestor to all 108 isolates existed in 2006 (1998-2010 95% CI relaxed exponential clock model) assuming a constant population size model (Figure S3). For the IncX4 backgrounds we dated the common ancestor of the eight isolates to 2011 (2010-2013 95% CI relaxed exponential clock model) assuming a constant population size model (Figure S6). Posterior density distributions of root dating under different population models are shown in Figures S2-S5. The difference in dating inferred for these two plasmid backgrounds and the recent date obtained for IncX4 highlight the dynamic nature of the integration of the *mcr-1* carrying transposon, even if in the IncX4 phylogeny isolates from East Asia and Europe and the Americas cluster together. The inferred mutation rates obtained for the IncI2 and IncX4 backgrounds consistently lie around $5\text{-}10 \times 10^{-5}$ substitutions per site per year (Table S1).

Environmental distribution of the composite mcr-1 transposon

It has been suggested that agricultural use of colistin, as has been widespread in China since the early 1980s²⁰, caused the initial emergence and spread of *mcr-1*^{24,25}. According to the evolutionary model in Figure 2, the ancestral mobilizable state is represented by the transposon carrying both its ISAp1 elements. The transposon is thought to lose its capability for mobilization after the loss of both ISAp1 elements¹², although a single copy is reportedly sufficient to keep some ability to mobilize, with the upstream copy being functionally more important. Comparing human (n=108) and non-human (n=252) isolates, there were significantly more sequences with some trace of the insertion sequence ISAp1 both upstream and downstream in non-human isolates (32/220 vs. 5/108, χ^2 test, $p=0.033$). This comparison held when only comparing agricultural isolates to human isolates (n=213) (28/213 vs. 5/108, χ^2 test, $p=0.029$). Furthermore, of the 42 isolates that had ISAp1 fragments both upstream and downstream, the majority were from Asia (n=30) with only a quarter from Europe (n=10) (χ^2 test, $p=0.12$). This result is not driven by an over-representation of agricultural isolates from Asia in our dataset (χ^2 test, $p=0.38$).

Discussion

We assembled a global dataset of 457 *mcr-1* positive sequenced isolates and could show that there was a single integration event of *mcr-1* into an IS*Ap11* composite transposon, followed by its subsequent spread between multiple genomic backgrounds. Our phylogenetic analyses suggest an age of insertion of *mcr-1* into the gene transposon shared across our isolates in the mid 2000s (2002-2008 95% HPD). We could identify the likely sequence of the ancestral transposon type and show the pattern of diversity supports a single mobilization with subsequent diversification during global spread.

Despite the limited number of whole genome sequences for samples before 2012, with the oldest sequence available from 2008 (Figure 1C), our estimate is consistent with the majority of available evidence from retrospective surveillance data²⁴ which has found the presence of *mcr-1* in samples dating back to 2005 in Europe²⁶. One retrospective study of Chinese isolates from 1970-2014 reported three *mcr-1* positive *E. coli* dating from the 1980s²⁷, although *mcr-1* then did not reappear until 2004. If valid, this isolated observation provides evidence only for the presence of *mcr-1* as a gene rather than in mobilizable form, which would be consistent with an early emergence but a long dormancy before the formation of the composite transposon, subsequent mobilization, and global spread. We found that a constant population size model gave a better fit than an exponential model, suggesting the dramatic increase in reports of the presence of *mcr-1* across the past two years may not reflect a sudden global spread after its initial discovery² and highlighting the difficulty of interpreting novel surveillance data from previously unknown resistance elements.

Our estimates of the age of spread of the representative IncI2 and IncX4 plasmid backgrounds are more recent, dating to around 2008 and 2013, respectively, but are both consistent with the age of the transposon mobilization event. We did not constrain the evolutionary rates in any of our phylogenetic analyses. It is thus encouraging that the different rates are highly consistent between the *mcr-1* transposon and the two plasmid backgrounds. While this points to high internal consistency between our estimates, we were surprisingly unable to find any previously published estimates for the evolutionary rate of bacterial plasmids.

The current distribution and observed genetic patterns are in line with a centre of origin in China. This is the place where we observe the highest proportion of isolates carrying intact or partial copies of the IS*Ap11* flanking elements. Transposon sequences carrying IS*Ap11* elements were also overrepresented in environmental and agriculture isolates, relative to those collected from humans. This pattern is in line with agricultural settings

acting as the source of *mcr-1* within bacteria isolated from humans²⁰. The current global distribution has been achieved through multiple translocations, and is illustrated by the interspersed geographic origins in our phylogenetic reconstructions. A likely driver for the global spread is trade, in particular food animals²⁸ and meat, although direct global movement by colonized or infected humans¹⁹ is also likely to have played a role in the current distribution.

The origin of *mcr-1* prior to its mobilization remains elusive. Despite an exhaustive search of sequence repositories, including the short-read archive, we found not a single *mcr-1* sequence outside the IS*Ap11* transposon background. IS*Ap11* was first identified in the pig pathogen *Actinobacillus pleuropneumoniae*²⁹ suggesting that it may also have been an ancestral host for *mcr-1*, although to our knowledge no *mcr-1* positive *A. pleuropneumoniae* isolates have been described. The phosphoethanolamine transferase (*EptA*) from *Paenibacillus sophorae* has also been proposed as a possible candidate³⁰. However, this seems most unlikely as *Paenibacilli* are gram positive and are thus intrinsically resistant to polymyxins³¹. Moreover, while the two sequences share functional similarities, this should be interpreted as a case of possible parallel evolution rather than direct filiation³¹. *Moraxella* has also been suggested as being the source of *mcr-1*³², following the identification of genes in *Moraxella* with limited homology to *mcr-1* (~60% nucleotide sequence identity). However, this sequence identity is too low for *Moraxella* to be considered as viable candidates for the origin of *mcr-1*. The search for the initial source of *mcr-1* remains open until a *mcr-1* sequence is identified outside of the IS*Ap11* sequence background.

We note that there are an increasing number of mobilized genes that can confer colistin resistance, with *mcr-2* reported less than a year after *mcr-1* was initially described³³ and more recently the phylogenetically distant *mcr-3*, *mcr-4*, and *mcr-5* have also been described^{34–36}. There appear to be commonalities between the mechanisms of the *mcr* genes, despite their different sequences and location near to different insertion sequences. For example, *mcr-2* has 76.7% nucleotide identity to *mcr-1* and was found in colistin-resistant isolates that did not contain *mcr-1*, and appeared to be mobilized on an IS1595 transposon³³. Despite the different insertion sequences, intriguingly, this mobile element also contained a similar protein downstream of the *mcr* gene. Indeed, in *mcr-1*, -2 and -3, the *mcr* gene has a downstream open reading frame encoding, respectively, a putative PAP2 protein¹², a PAP2 membrane-associated lipid phosphatase³³, and a diacylglycerol kinase³⁴, all of which have transmembrane domains and are involved in the phosphatidic acid pathway^{37,38}. While the PAP2-like orf in *mcr-1* has been shown to not be required for colistin resistance³⁹, the presence of similar sequences downstream of other *mcr* genes implies some functional role, either in the formation of the mobile element and/or in its continued mobilization.

In summary, we assembled the largest dataset to date on *mcr-1* positive sequenced samples through our own sequencing efforts combined with an exhaustive search of *mcr-1* positive isolates sequenced and deposited on publicly available databases including unassembled datasets from the SRA. While this allowed us to obtain a truly global dataset of 457 *mcr-1* positive isolates covering 31 countries and five continents, we appreciate that the data is likely affected by complex sampling biases, with an overrepresentation of samples from places with active surveillance and well-funded research communities. Equally, although we took advantage of the most sophisticated bioinformatics and phylogenetic tools currently available, the complex “Russian doll” dynamics of the transposon, plasmids, and bacterial host limits our ability to reach strong inferences on some important aspects of the spread of *mcr-1*. Nevertheless, we believe our results highlight the potential for phylogenetic reconstruction of antimicrobial resistance elements at a global scale. We hope that future efforts relying on more sophisticated computational tools and even more extensive genetic sequence data will become part of the routine toolbox in infectious disease surveillance.

Methods

Compilation of genomic dataset

We blasted for *mcr-1* in all NCBI GenBank assemblies (as of 16th March 2017, $n=90,759$) using a 98% identity cut off. 195 records (0.21%; 121 assemblies, 73 complete plasmids, 1 complete chromosome) contained at least one contig with a full-length hit to *mcr-1* (1,626 bases). We only included samples with a single copy of *mcr-1*.

We searched a snapshot of all whole-genome sequenced bacterial raw read datasets in the SRA (December 2016), looking for samples containing *mcr-1* by using a k-mer-index which we had previously constructed ($k=31$, software available at: <https://github.com/phelimbc/cbg>). This snapshot consisted of 455,632 samples, of which 7,799 were excluded as they exceeded an arbitrary threshold of 10 million k-mers after error-cleaning with McCortex⁴⁰. 184 datasets were found to contain at least 70% of the 31-mers in *mcr-1*. After removing duplicates (i.e. those with a draft assembly available) we could assemble contigs with *mcr-1* for 153 of these.

Our final dataset comprised 457 isolates from six genera across 31 different countries, ranging in date from 2008 to 2017. Where only a year was provided as the date of isolate collection the date was set to the midpoint of that year.

Whenever identified isolates did not comprise previously assembled genomes or complete plasmids, the raw fastq files were first inspected using FastQC and trimmed and filtered on a case by case basis. De-novo assembly was then conducted using Plasmid SPADES 3.10.0 using the *--careful* switch and otherwise default parameters⁴¹. For those isolates sequenced using PacBio a different pipeline was employed. Correction, trimming and assembly of raw reads was performed using Canu⁴² and assembled reads were corrected and trimmed using the tool Circlator⁴³. The quality of resultant assemblies was assessed using infseq. In both cases the *mcr-1* carrying contigs in this final dataset were identified using blastn v2.2.31⁴⁴.

We ran Plasmid Finder 1.3⁴⁵ with 95% identity to identify plasmid replicons on the *mcr-1* carrying contigs. 177 contigs could be assigned a plasmid type using this method.

Novel samples from China

We selected 110 *mcr-1* positive isolates from China for whole genome sequencing from a larger survey effort of both clinical and livestock isolates. 2,824 non-repetitive clinical isolates, including 1,637 *E. coli* and 1,187 *K. pneumoniae* were collected from 15

provinces of mainland China from 2011 to 2016. 72 isolates were resistant to polymyxin B, comprising 40 *E. coli* and four *K. pneumoniae* carrying *mcr-1*. Livestock samples were collected from four provinces of China in 2013 and 2016. One broiler farm of the Shandong province provided chicken anal swabs, liver, heart and wastewater isolated in 2013. In 2016, samples including faeces, wastewater, anal swabs, and internal organs of sick livestock were collected from swine farms, cattle farms and broiler farms in four provinces (Jilin, Shandong, Henan and Guangzhou). A total of 601 *E. coli* and 126 *K. pneumoniae* were isolated, of which 167 (137 *E. coli* and 30 *K. pneumoniae*) were resistant to polymyxin B. We detected *mcr-1* in 135 *E. coli* and two *K. pneumoniae*, as well as in eight *E. coli* isolated from environmental samples, which were collected from influents and effluents of four tertiary care teaching hospitals.

All of the isolates were sent to the microbiology laboratory of Peking University People's Hospital and confirmed by routine biochemical tests, the Vitek system (bioMérieux, Hazelwood, MO) and/or MALDI-TOF (Bruker Daltonics, Bremen, Germany). The minimal inhibitory concentrations (MICs) of polymyxin B was determined using the broth dilution method. The breakpoints of polymyxin B for Enterobacteriaceae were interpreted with the European Committee on Antimicrobial Susceptibility Testing (EUCAST, http://www.eucast.org/clinical_breakpoints) guidelines. Colistin-resistant isolates (MIC of ≥ 2 $\mu\text{g/ml}$) were screened for *mcr-1* by PCR and sequencing as described previously⁴⁶.

Identification and alignment of mcr-1 transposon

We searched for the *mcr-1* carrying transposon region across isolates by blasting for its major components: IS*Apl1* (*Actinobacillus pleuropneumoniae* reference sequence: EF407820), *mcr-1* (from *E. coli* plasmid pHNSHP45: KP347127.1), and short sequences representing the sequences immediately upstream and downstream of *mcr-1* (from KP347127.1) using blastn-short. Contiguous sequences containing *mcr-1* were aligned using Clustal Omega⁴⁷ and then manually curated and amended using Jalview⁴⁸, resulting in a 3,679bp alignment containing the common ~2,600bp identified by Snesrud and colleagues¹². The downstream copy of IS*Apl1* was more often fragmented or inverted. 28 isolates which were all assemblies from the same study in Vietnam had a ~1.7kb insertion downstream of *mcr-1* (Figure 3e) before the downstream IS*Apl1* element.

Phylogenetic analyses

For constructing the transposon phylogeny, we excluded the downstream IS*Apl1* and the insertion sequence observed in a small number of samples, as well as regions identified as having signals of recombination by ClonalFrameML⁴⁹, resulting in a

3,522bp alignment. We removed two homoplastic sites (requiring >1 change on the phylogeny), before constructing a maximum parsimony neighbor-joining tree based on the Hamming distance between sequences. We calculated branch lengths using non-negative least squares with `npls.phylo` in `phangorn v2.2.0`⁵⁰. Phylogenies were visualized with `ggtree v1.8.1`⁵¹.

Phylogenetic dating

Given recombination can conceal the clonal phylogenetic signal we also applied `ClonalFrameML`⁴⁹ to identify regions of high recombination in a subset of `Incl2` and `IncX4` plasmid background alignments. Where recombination hotspots were identified, they were removed from the alignment. In the `Incl2` alignment this resulted in removing 1,281 positions. No regions of high recombination were detected in the `IncX4` alignment. We applied root-to-tip correlations to test for a temporal signal in the data using `TempEST`⁵². There was a significantly positive slope for all three alignments (Fig. S7-S9).

We applied `BEAUTi` and `BEAST v2.4.7`^{53,54} to estimate a timed phylogeny from an alignment of `Incl2` plasmids (7,161 sites, 110 isolates) and `IncX4` plasmids (34,761 sites, 8 isolates). Sequences were annotated using their known sampling times expressed in years. For both plasmid alignments, the HKY substitution model was selected based on evaluation of all possible substitution models in `bModelTest`. `Beast` analyses were then applied under both a coalescent population model (the coalescent Bayesian skyline implementation) and an exponential growth model (Coalescent Exponential population implementation). Additionally, a strict clock, with a lognormal prior, and a relaxed clock (both lognormal and exponential) were tested. MCMC was run for 50,000,000 iterations sampling every 2000 steps and convergence was checked by inspecting the effective sample sizes (ESS) and parameter value traces in the software `Tracer v1.6.0`. Analyses were repeated three times to ensure consistency between the obtained posterior distributions. Posterior trees for the best fitting model were combined in `TreeAnnotator` after a 10% burn-in to provide an annotated Maximum Clade Credibility (MCC) tree. MCC trees were plotted using `ggtree`⁵¹ for both backgrounds: `Incl2` (Figure S10) and `IncX4` (Figure S11). The model fit across analyses was compared using the Akaike's information criteria model (AICM) through 100 boot-strap resamples as described in Baele and colleagues⁵⁵ and implemented in `Tracer v1.6` (Table S2).

Phylogenetic dating on the transposon was performed using an alignment of 364 isolates, which included only those with information on isolation date, across 3,522 sites. As before `Beast` analyses were applied under both a coalescent population model (coalescent Bayesian skyline implementation) and an exponential growth model

(coalescent exponential population implementation). Additionally, a strict clock, with a lognormal prior, and a relaxed clock (both lognormal and exponential) were tested. Analyses were run under a HKY substitution model for 600 million iterations sampling every 5,000 steps. Only analyses using a strict clock model reached convergence after 600 million iterations. The resultant set of trees were thinned by sampling every 10 trees and excluding a 10% burn-in and combined using TreeAnnotator to produce a MCC tree. MCC trees were plotted using ggTree⁴⁸. As before the model fit was evaluated using AICM's implemented in Tracer v1.6.

Environmental distribution

For the purpose of testing the distribution of sequences containing some trace of ISAp11, we classed isolates into broad categories as either environmental (n=39; bird, cat, dog, fly, food, penguin, reptile, vegetables), agricultural (n=213; chicken, cow, pig, poultry feed, sheep, turkey), or human (n=108).

Acknowledgments

L.v.D., X.D., H.W., T.S., L.A.W. and FB acknowledge financial support from the Newton Trust UK-China NSFC initiative (grants MR/P007597/1 and 81661138006). F.B. additionally acknowledges support from the BBSRC GCRF scheme. L.S. was supported by a PhD scholarship from EPSRC (EP/F500351/1). P.B. is funded by Wellcome Trust on a "Genomic Medicine and Statistics DPhil" grant. A.R. was co-funded by the European Union: European regional development fund (ERDF), by the Conseil Régional de La Réunion and by the Centre de Coopération internationale en Recherche agronomique pour le Développement (CIRAD). H.W. was supported by National Natural Science Foundation of China (81625014). L.A.W. is supported by a Dorothy Hodgkin Fellowship funded by the Royal Society (Grant Number DH140195) and a Sir Henry Dale Fellowship jointly funded by the Wellcome Trust and the Royal Society (Grant Number 109385/Z/15/Z). The funders had no role in study design, data collection and interpretation, or the decision to submit the work for publication.

Data access

The 110 *mcr-1* positive Illumina sequencing data have been submitted to the Short Read Archive under Bioproject: [PRJNA408214](#), Accession: SRP118547. The data will be released upon peer-reviewed publication or on the 2018-9-21.

Contributions

H.W., and F.B. conceived the project and designed the experiments. R.W., Q.W., X.W., L.J. Q.Z., Y.L and H.W collected samples. R.W., Q.W., X.W., L.J., Q.Z., and Y.L performed microbial identification, antimicrobial susceptibility testing, screening for *mcr-1*, and DNA extraction for WGS. R.W. L.V.D., L.S. assembled the new sequence data. L.v.D. and L.S. curated the global dataset and performed the computational analyses. T.D.S. advised on functional aspects of colistin resistance. A.R, L.A.W. and X.D. helped with the phylogenetic reconstructions. P.B. and Z.I. performed the search for *mcr-1* positive samples on the Short Read Archive. H.W. takes responsibility for the accuracy and availability of the epidemiological and raw sequence data, and F.B. for all bioinformatics and computational methods and results. L.v.D., L.S. and F.B. wrote the paper with contributions from X.D. and H.W.. All authors read and commented on successive drafts and all approved the content of the final version. Z.I. was funded by a Sir Henry Dale Fellowship jointly funded by the Wellcome Trust and the Royal Society (Grant Number 102541/Z/13/Z)

Competing interests

The authors declare no competing financial interests.

Literature

1. Grégoire, N., Aranzana-Climent, V., Magréault, S., Marchand, S. & Couet, W. Clinical Pharmacokinetics and Pharmacodynamics of Colistin. *Clin. Pharmacokinet.* (2017). doi:10.1007/s40262-017-0561-1
2. Liu, Y.-Y. *et al.* Emergence of plasmid-mediated colistin resistance mechanism MCR-1 in animals and human beings in China: a microbiological and molecular biological study. *Lancet Infect. Dis.* **16**, 161–168 (2016).
3. Olaitan, A. O., Morand, S. & Rolain, J.-M. Mechanisms of polymyxin resistance: acquired and intrinsic resistance in bacteria. *Front. Microbiol.* **5**, 643 (2014).
4. Lee, J.-Y., Choi, M.-J., Choi, H. J. & Ko, K. S. Preservation of Acquired Colistin Resistance in Gram-Negative Bacteria. *Antimicrob. Agents Chemother.* **60**, 609–612 (2016).
5. Carattoli, A. Plasmids and the spread of resistance. *Int. J. Med. Microbiol.* **303**, 298–304 (2013).
6. Poirel, L., Kieffer, N., Liassine, N., Thanh, D. & Nordmann, P. Plasmid-mediated carbapenem and colistin resistance in a clinical isolate of *Escherichia coli*. *Lancet Infect. Dis.* **16**, 281 (2016).
7. Du, H., Chen, L., Tang, Y.-W., Kreiswirth, B. N. & Rolain, J.-M. Emergence of the *mcr-1* colistin resistance gene in carbapenem-resistant Enterobacteriaceae. *Lancet Infect. Dis.* **16**, 287–288 (2016).
8. Yao, X., Doi, Y., Zeng, L., Lv, L. & Liu, J.-H. Carbapenem-resistant and colistin-resistant *Escherichia coli* co-producing NDM-9 and MCR-1. *Lancet Infect. Dis.* **16**, 288–289 (2016).
9. Zhang, X.-F. *et al.* Possible Transmission of *mcr-1* –Harboring *Escherichia coli* between Companion Animals and Human. *Emerg. Infect. Dis.* **22**, 1679–1681 (2016).
10. Falgenhauer, L. *et al.* Colistin resistance gene *mcr-1* in extended-spectrum β -lactamase-producing and carbapenemase-producing Gram-negative bacteria in Germany. *Lancet Infect. Dis.* **16**, 282–283 (2016).
11. Haenni, M. *et al.* Co-occurrence of extended spectrum β lactamase and MCR-1 encoding genes on plasmids. *Lancet Infect. Dis.* **16**, 281–282 (2016).
12. Snesrud, E. *et al.* A Model for Transposition of the Colistin Resistance Gene *mcr-1* by ISAp11. *Antimicrob. Agents Chemother.* **60**, 6973–6976 (2016).
13. Wang, Y. *et al.* Comprehensive resistome analysis reveals the prevalence of NDM and MCR-1 in Chinese poultry production. *Nat. Microbiol.* **2**, 16260 (2017).
14. Li, R. *et al.* Genetic characterization of *mcr-1* -bearing plasmids to depict molecular mechanisms underlying dissemination of the colistin resistance determinant. *J. Antimicrob. Chemother.* **72**, 393–401 (2017).
15. Matamoros, S. *et al.* Global Phylogenetic Analysis Of *Escherichia coli* And

- Plasmids Carrying The *mcr-1* Gene Indicates Bacterial Diversity But Plasmid Restriction. *bioRxiv* 136804 (2017). doi:10.1101/136804
16. Zhou, H.-W. *et al.* Occurrence of Plasmid- and Chromosome-Carried *mcr-1* in Waterborne Enterobacteriaceae in China. *Antimicrob. Agents Chemother.* **61**, e00017-17 (2017).
 17. Yang, D. *et al.* The Occurrence of the Colistin Resistance Gene *mcr-1* in the Haihe River (China). *Int. J. Environ. Res. Public Health* **14**, 576 (2017).
 18. Fernandes, M. R. *et al.* Colistin-Resistant *mcr-1* -Positive *Escherichia coli* on Public Beaches, an Infectious Threat Emerging in Recreational Waters. *Antimicrob. Agents Chemother.* **61**, e00234-17 (2017).
 19. von Wintersdorff, C. J. H. *et al.* Detection of the plasmid-mediated colistin-resistance gene *mcr-1* in faecal metagenomes of Dutch travellers. *J. Antimicrob. Chemother.* **71**, 3416–3419 (2016).
 20. Wang, Y. *et al.* Prevalence, risk factors, outcomes, and molecular epidemiology of *mcr-1*-positive Enterobacteriaceae in patients and healthy adults from China: an epidemiological and clinical study. *Lancet. Infect. Dis.* **17**, 390–399 (2017).
 21. Sheppard, A. E. *et al.* Nested Russian Doll-Like Genetic Mobility Drives Rapid Dissemination of the Carbapenem Resistance Gene *blaKPC*. *Antimicrob. Agents Chemother.* **60**, 3767–78 (2016).
 22. Snesrud, E. *et al.* Analysis of Serial Isolates of *mcr-1* -Positive *Escherichia coli* Reveals a Highly Active IS *Apl1* Transposon. *Antimicrob. Agents Chemother.* **61**, e00056-17 (2017).
 23. Poirel, L. *et al.* Genetic Features of MCR-1-Producing Colistin-Resistant *Escherichia coli* Isolates in South Africa. *Antimicrob. Agents Chemother.* **60**, 4394–7 (2016).
 24. Poirel, L. & Nordmann, P. Emerging plasmid-encoded colistin resistance: the animal world as the culprit? *J. Antimicrob. Chemother.* **71**, 2326–2327 (2016).
 25. Schwarz, S. & Johnson, A. P. Transferable resistance to colistin: a new but old threat. *J. Antimicrob. Chemother.* **71**, 2066–70 (2016).
 26. Haenni, M. *et al.* Co-occurrence of extended spectrum β lactamase and MCR-1 encoding genes on plasmids. *Lancet Infect. Dis.* **16**, 281–282 (2016).
 27. Shen, Z., Wang, Y., Shen, Y., Shen, J. & Wu, C. Early emergence of *mcr-1* in *Escherichia coli* from food-producing animals. *Lancet. Infect. Dis.* **16**, 293 (2016).
 28. Grami, R. *et al.* Impact of food animal trade on the spread of *mcr-1* -mediated colistin resistance, Tunisia, July 2015. *Eurosurveillance* **21**, 30144 (2016).
 29. Tegetmeyer, H. E., Jones, S. C. P., Langford, P. R. & Baltes, N. IS*Apl1*, a novel insertion element of *Actinobacillus pleuropneumoniae*, prevents ApxIV-based serological detection of serotype 7 strain AP76. *Vet. Microbiol.* **128**, 342–353 (2008).
 30. Gao, R. *et al.* Dissemination and Mechanism for the MCR-1 Colistin Resistance. *PLOS Pathog.* **12**, e1005957 (2016).

31. Di Conza, J. A., Radice, M. A. & Gutkind, G. O. MCR1: rethinking the origin. *Int. J. Antimicrob. Agents* (2017). doi:10.1016/j.ijantimicag.2017.06.003
32. Kieffer, N., Nordmann, P. & Poirel, L. Moraxella Species as Potential Sources of MCR-Like Polymyxin Resistance Determinants. *Antimicrob. Agents Chemother.* **61**, (2017).
33. Xavier, B. B. *et al.* Identification of a novel plasmid-mediated colistin-resistance gene, *mcr-2*, in *Escherichia coli*, Belgium, June 2016. *Euro Surveill.* **21**, 30280 (2016).
34. Yin, W. *et al.* Novel Plasmid-Mediated Colistin Resistance Gene *mcr-3* in *Escherichia coli*. *MBio* **8**, e00543-17 (2017).
35. Carattoli, A. *et al.* Novel plasmid-mediated colistin resistance *mcr-4* gene in *Salmonella* and *Escherichia coli*, Italy 2013, Spain and Belgium, 2015 to 2016. *Eurosurveillance* **22**, 30589 (2017).
36. Borowiak, M. *et al.* Identification of a novel transposon-associated phosphoethanolamine transferase gene, *mcr-5*, conferring colistin resistance in d-tartrate fermenting *Salmonella enterica* subsp. *enterica* serovar Paratyphi B. *J. Antimicrob. Chemother.* (2017). doi:10.1093/jac/dkx327
37. Athenstaedt, K. & Daum, G. Phosphatidic acid, a key intermediate in lipid metabolism. *Eur. J. Biochem.* **266**, 1–16 (1999).
38. Epanand, R. M., Walker, C., Epanand, R. F. & Magarvey, N. A. Molecular mechanisms of membrane targeting antibiotics. *Biochim. Biophys. Acta - Biomembr.* **1858**, 980–987 (2016).
39. Zurfluh, K., Kieffer, N., Poirel, L., Nordmann, P. & Stephan, R. Features of the *mcr-1* Cassette Related to Colistin Resistance. *Antimicrob. Agents Chemother.* **60**, 6438–9 (2016).
40. Turner, I., Garimella, K. V., Iqbal, Z. & McVean, G. Integrating long-range connectivity information into de Bruijn graphs. *doi.org* 147777 (2017). doi:10.1101/147777
41. Antipov, D. *et al.* plasmidSPAdes: assembling plasmids from whole genome sequencing data. *Bioinformatics* **32**, 3380–3387 (2016).
42. Koren, S. *et al.* Canu: scalable and accurate long-read assembly via adaptive k-mer weighting and repeat separation. *Genome Res.* gr.215087.116 (2017). doi:10.1101/gr.215087.116
43. Hunt, M. *et al.* Circlator: automated circularization of genome assemblies using long sequencing reads. *Genome Biol.* **16**, 294 (2015).
44. Camacho, C. *et al.* BLAST+: architecture and applications. *BMC Bioinformatics* **10**, 421 (2009).
45. Carattoli, A. *et al.* In silico detection and typing of plasmids using PlasmidFinder and plasmid multilocus sequence typing. *Antimicrob. Agents Chemother.* **58**, 3895–903 (2014).
46. Wang, X. *et al.* Molecular epidemiology of colistin-resistant Enterobacteriaceae in

- inpatient and avian isolates from China: high prevalence of mcr-negative *Klebsiella pneumoniae*. *Int. J. Antimicrob. Agents* **50**, 536–541 (2017).
47. Sievers, F. *et al.* Fast, scalable generation of high-quality protein multiple sequence alignments using Clustal Omega. *Mol. Syst. Biol.* **7**, 539 (2011).
 48. Waterhouse, A. M., Procter, J. B., Martin, D. M. A., Clamp, M. & Barton, G. J. Jalview Version 2--a multiple sequence alignment editor and analysis workbench. *Bioinformatics* **25**, 1189–91 (2009).
 49. Didelot, X. & Wilson, D. J. ClonalFrameML: efficient inference of recombination in whole bacterial genomes. *PLoS Comput. Biol.* **11**, e1004041 (2015).
 50. Schliep, K. P. phangorn: phylogenetic analysis in R. *Bioinformatics* **27**, 592–3 (2011).
 51. Yu, G., Smith, D. K., Zhu, H., Guan, Y. & Lam, T. T.-Y. ggtree: an r package for visualization and annotation of phylogenetic trees with their covariates and other associated data. *Methods Ecol. Evol.* **8**, 28–36 (2017).
 52. Rambaut, A., Lam, T. T., Max Carvalho, L. & Pybus, O. G. Exploring the temporal structure of heterochronous sequences using TempEst (formerly Path-O-Gen). *Virus Evol.* **2**, vew007 (2016).
 53. Drummond, A. J., Suchard, M. A., Xie, D. & Rambaut, A. Bayesian Phylogenetics with BEAUti and the BEAST 1.7. *Mol. Biol. Evol.* **29**, 1969–1973 (2012).
 54. Bouckaert, R. *et al.* BEAST 2: a software platform for Bayesian evolutionary analysis. *PLoS Comput. Biol.* **10**, e1003537 (2014).
 55. Baele, G. *et al.* Improving the accuracy of demographic and molecular clock model comparison while accommodating phylogenetic uncertainty. *Mol. Biol. Evol.* **29**, 2157–67 (2012).